

# Emittance Measurement at the NSLS X-Ray Ring\*

J. Safranek and P.M. Stefan

National Synchrotron Light Source, Brookhaven National Laboratory, Upton, NY 11973

## Abstract

A pinhole camera for imaging x-ray synchrotron radiation from a dipole magnet is now in operation at the NSLS X-Ray Ring. The pinhole camera detector is a 0.5 mm thick YAG phosphor screen viewed by a video camera. Both the theoretical pinhole diffraction pattern and the measured modulation transfer function (MTF) of the phosphor and camera have been deconvolved from the measured profile in order to derive the true transverse profile of the electron beam. This profile was then fit to a 2-dimensional Gaussian. The electron beam emittance as a function of the phase space acceptance of the pinhole camera has been derived, so the horizontal and vertical electron emittances can be deduced from the major and minor sigmas of the fit Gaussian. In the X-Ray Ring, the vertical emittance is kept small to maximize the synchrotron radiation brightness. The ratio of the measured vertical to horizontal emittance is 0.001.

## 1 INTRODUCTION

Prior to this work, the NSLS X-Ray Ring had a transverse beam profile monitor which imaged visible synchrotron radiation. Due to diffraction effects, however, this monitor was unable to resolve the small vertical beam size [1] that has been achieved in the X-Ray Ring. With a push toward smaller beam size and higher brightness synchrotron radiation, a higher resolution profile monitor was needed, so a dedicated x-ray pinhole camera was built. This diagnostic is now available to monitor the beam size during operations.

## 2 THE MEASUREMENT HARDWARE

Pinhole: A rectangular pinhole was made from a horizontal and a vertical molybdenum slit. To minimize x-ray scatter and reflection from the slit jaws, the slit gaps were tapered 5 degrees so that the gaps at the upstream end of the slits are slightly smaller than those downstream. The molybdenum jaws for each slit are 3.2 mm thick, which is sufficient to stop most of the x-ray spectrum from the 2.5 GeV NSLS X-Ray Ring. The gaps of the slits were adjusted to about 30  $\mu\text{m}$  in order to minimize the width of the x-ray diffraction pattern and so maximize the pinhole camera resolution. The exact dimensions of the gaps were deduced from the diffraction pattern created by the slits when illuminated

with a HeNe laser. The pinhole is located 7.54 m from the x-ray source point, and a YAG phosphor screen is located an additional 9.27 m downstream of the pinhole.

Detector: The profile on the YAG phosphor is imaged with a 50 mm focal length Nikon lens attached with a bellows to a Pulnix TM-745 CCD video camera. The lens is positioned to give a factor of 2.4 magnification between the phosphor and the CCD. The video signal is digitized and displayed with a Spiricon LBA-100A Laser Beam Analyzer.

## 3 RESOLUTION AND MTF

In order to accurately derive the electron beam emittance from the measured pinhole camera intensity profile, the resolution functions of the setup should be removed. There are two resolution functions associated with this measurement: 1) the resolution of the phosphor and video camera system and 2) the diffraction pattern from the pinhole for an ideal point source.

Phosphor and Video Camera: The combined resolution of the phosphor, lens and video camera was measured by placing a very thin slit (a  $\delta$ -function) just in front of the phosphor. The resulting profile, digitized by the Spiricon, is shown with a solid line in figure 1. The amplitude part the FFT of this profile gives the modulation transfer function (MTF) of the detector. This is simply a measure of the relative attenuation of the spatial frequencies and is shown in figure 2.

Pinhole camera: Low energy photons are filtered out by a 250  $\mu\text{m}$  thick beryllium window and a 25  $\mu\text{m}$  aluminum foil at the end of the beam line, just upstream of the phosphor. The pinhole diffraction pattern is neither far field nor a geometric image, but something between the two. The diffraction pattern was calculated numerically for each of many energies over the synchrotron radiation spectrum absorbed by the YAG phosphor, and a weighted sum was taken to calculate the diffraction pattern for the full spectrum (dotted line in figure 1). The FFT was taken to yield the pinhole camera MTF (dotted line in figure 2).

Deconvolving the resolution functions: In order to derive the true profile of the electron beam, the pinhole diffraction pattern and the measured video camera resolution need to be deconvolved from the measured profile. Deconvolution is easiest in the frequency domain where it simply becomes division (see, for example, [4]). Rather than include both the phase and amplitude of each spatial frequency of the resolution function, a common procedure

\* Work performed under the auspices of the U.S. Department of Energy

in image analysis is to throw out the phase part and divide only by the amplitude part of the FFT of the resolution function. As mentioned above, this amplitude part is called the modulation transfer function MTF. For a symmetric response function, the phase is the same for all spatial frequencies, so throwing out the phase does not change the result. Throwing out the phase simply filters out some of the noise in the response function measurement.

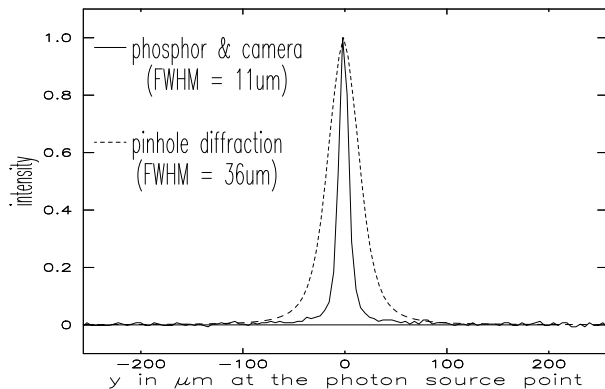


Figure 1: There are two contributions to the resolution of the beam size measurement – pinhole diffraction and the resolution of the phosphor/video camera combination.

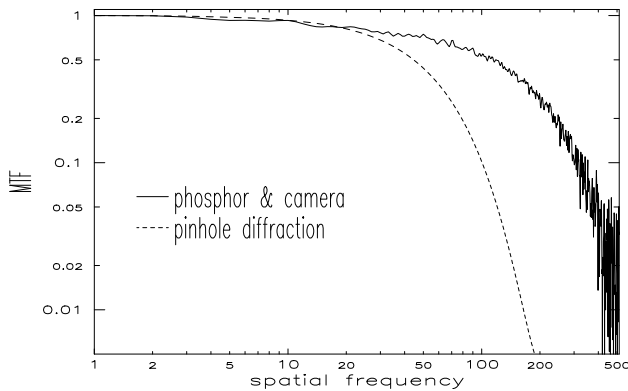


Figure 2: MTF associated with each of the resolution functions shown in figure 1.

Figure 3 shows a vertical slice through the beam profile. The raw measured data is plotted as well as the profile after removing noise and deconvolving the two resolution functions shown in figure 1. Figure 4 shows the amplitudes of the spatial frequencies for each of these profiles. Deconvolution enhances the higher spatial frequencies. Spatial frequencies in the raw data above about the 70<sup>th</sup> spatial frequency are clearly noise. These spatial frequencies were removed to avoid amplifying noise when deconvolving.

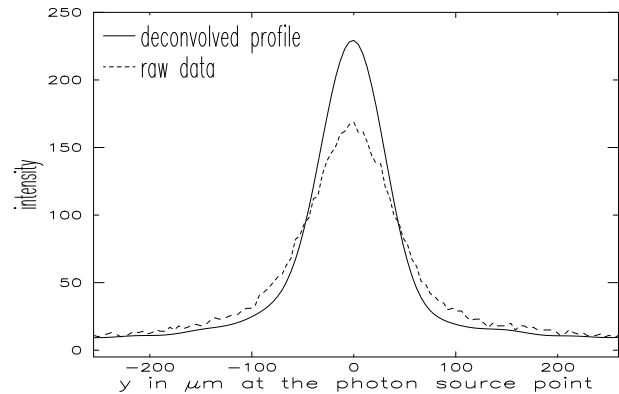


Figure 3: Vertical slice through the measured profile, before and after deconvolution. The skew quadrupoles were set to minimize the vertical size.

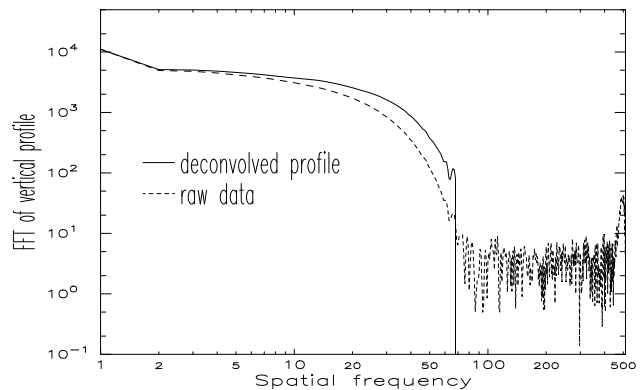


Figure 4: FFT spatial frequency amplitude for profiles shown in figure 3.

## 4 EMITTANCE MEASUREMENT

Define  $L1$  as the distance from the photon beam source point to the pinhole and define  $L2$  as the distance from the pinhole to the phosphor screen. The electron beam in a dipole does not radiate uniformly in  $4\pi$  steradians, so the image made by a pinhole camera is not necessarily simply the the electron beam distribution magnified by  $L2/L1$ . (I will show in what follows that this simple formula does in fact give the correct result to a good approximation in the horizontal plane, but not in general in the vertical plane.) To understand exactly what is imaged by the pinhole camera, one must consider the photon distribution in  $(x, x', y, y')$  phase space. The photon distribution is given by the convolution of the electron distribution with the photon distribution from a single electron.

Figure 5 shows graphs of the  $e^{-0.5}$  ellipses for the electron and photon phase space in both the horizontal and vertical planes. The electron ellipse drawn is somewhat larger than the ellipse  $\gamma x^2 + 2\alpha x x' + \beta x'^2$ , because it also includes the effects of finite  $\eta$  and  $\eta'$ . Also shown in figure 5 is the line in phase space that defines the acceptance of the pinhole. These graphs were made for the radiation opening

angle ( $\sigma_{r'}$ ) corresponding to 9 keV photons, which is the peak of the spectrum absorbed by the YAG phosphor.

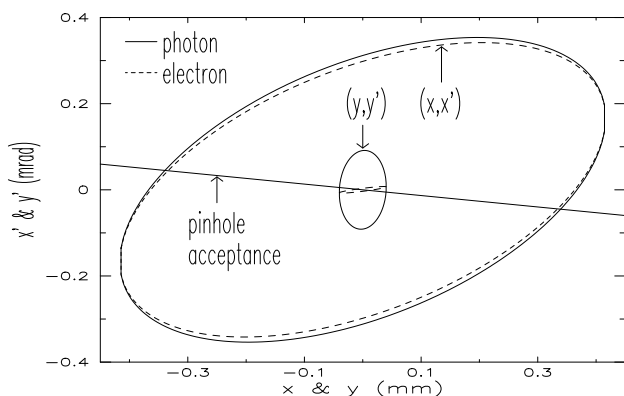


Figure 5: The phase space ellipses for the electron and photon beams in both the horizontal and vertical transverse dimensions. The electron phase ellipse as drawn includes the effects of finite  $\eta$  and  $\eta'$ . The vertical profile shown is measured with the skew quadrupoles adjusted to minimize the vertical emittance

**Vertical emittance:** Figure 5 shows that the pinhole happens to accept photons from about the full extent in  $y$  of electron beam. This means that, for this measurement, the simple formula for a pinhole camera is applicable: the vertical size of the image at the phosphor is simply  $L2/L1$  times the vertical electron beam size. This formula, however, does not hold in general in  $y$ . For example, it would give a factor of 2.5 too small an emittance if applied when measuring the vertical beam size in the X-Ray Ring with all the skew quadrupoles turned off. The solution that is correct in general can be found by equating the measured source distribution,  $\sigma_y$ , to the intersection of the pinhole camera acceptance and the photon ellipse plotted in figure 5. Doing this gives the emittance as a function of  $\alpha, \beta, \gamma, \epsilon, \eta, \eta', \sigma_\delta, \sigma_{r'}$  and  $L1$ . The parameters  $\alpha, \beta$ , and  $\gamma$  are known to a small fraction of a percent in the X-Ray Ring [2, 3], and the values of  $\eta$  and  $\eta'$  can be determined from the measured  $\eta$  at the two electron beam position monitors closest to the photon source point. Therefore,  $\epsilon$  can be accurately determined.

**Horizontal emittance:** In the  $(x, x')$  plane one must consider that the electron beam is following a curved trajectory in the dipole magnet. This means that the horizontal phase space ellipse sweeps across the pinhole acceptance in an arc in  $(x, x')$ . The extent of the arc in  $x$  is small, so to good approximation the ellipse sweeps linearly in  $x'$  along the line  $x = 0$  across the pinhole acceptance. The profile seen at the phosphor varies with time as the electron beam trajectory traverses an arc in the dipole. Analysis has shown that [6], despite the fact that at any given point on the electron beam trajectory through the dipole the pinhole does not accept photons from the whole extent of the beam in  $x$ , the time-integrated profile seen by the pinhole camera is the full horizontal distribution of the electrons. Therefore,

using the simple pinhole camera formula which gives the size at the phosphor as  $L2/L1$  times the electron beam size is a good approximation in  $x$ . Since  $\beta$  is well known [2, 3], and  $\eta$  can be determined from measurements at the electron beam position monitors, the horizontal emittance can be measured without ambiguity.

## 5 MEASUREMENT RESULTS

Table 1 shows the results of the emittance measurements with the x-ray pinhole camera. Both the horizontal and vertical emittance measurements show good agreement with the model.

Table 1.

	measured	model[2, 3]
Horizontal emittance	94.2 nm*rad	93.3 nm*rad
Vertical emittance (skew quadrupoles off)	8.6 nm*rad	6.6 nm*rad
Vertical emittance (skew quadrupoles on)	.1 nm*rad	—

## 6 ACKNOWLEDGEMENTS

Joe Rogers provided a good prototype design for the pinhole camera. One author owes a lot to Mike Sansone, Steve Sutton, and Mark Rivers for helping me make pinhole camera measurements on their beamlines prior to the construction of the dedicated pinhole camera and for giving me much useful advice. Thanks to Dean Chapman for letting me use his computer code for calculating the photon distribution absorbed by the phosphor. Thanks to John Dunsmuir for the lesson on MTF. Thanks to Mike Borland useful discussions concerning pinhole cameras. Thanks to Sam Krinsky for advice and for help editing. In addition, many other NSLS staff members gave useful advice to a neophyte of x-ray beamlines. Thanks.

## 7 REFERENCES

- [1] J. Safranek and S. Krinsky, Coupling Correction Using Closed Orbit Measurements, AIP Conference Proceedings, Vol 315, 1994.
- [2] J. Safranek and M.J. Lee, Calibration of the X-Ray Ring Quadrupoles, BPMs, and Orbit Correctors Using the Measured Orbit Response Matrix, AIP Conference Proceedings, Vol 315, 1994.
- [3] J. Safranek, Proc. 1995 IEEE Particle Accelerator Conference, (1995)
- [4] W. Press, B. Flannery, S. Teukolsky, W. Vetterling, Numerical Recipes, Cambridge, 1990.
- [5] G.K. Green, Spectra and Optics of Synchrotron Radiation, BNL 50522, 1976.
- [6] J. Safranek, to be published.